Calculation of $n=3$ intrashell resonance states of He^- and of isoelectronic atoms

Nicos A. Piangos[1,*] and Cleanthes A. Nicolaides[1,2,†]
[1]*Theoretical and Physical Chemistry Institute, National Hellenic Research Foundation, 48 Vasileos Constantinou Avenue, Athens 11635, Greece*
[2]*Physics Department, National Technical University, Athens, Greece*
(Received 22 October 2002; published 13 May 2003)

We discuss the theory and computation of the lowest three, $n=3$ intrashell triply excited resonance states of He^- of Li, and of positive ions of the sequence, up to N^{4+}. These are the $3s^2 3p\ ^2P^o$, $3s3p^2\ ^4P$, and $3s3p^2\ ^2D$ states, for which wave function characteristics, energies, and widths are reported. Contrary to recently published results for He^- and to earlier ones for N^{4+}, we found that electron correlation and orthogonality to lower states are such that they make the $^2P^o$ state the lowest $n=3$ triply excited state (TES), as is the case with the $n=2$ shell. Our predictions for these states of He^- are in harmony with the measurements of Roy [Phys. Rev. Lett. **38**, 1062 (1977)], which were interpreted only recently [C. A. Nicolaides and N. A. Piangos, J. Phys. B **34**, 99 (2001)]. In addition, our value for the position of the Li $3s^2 3p\ ^2P^o$ TES, 175.15 eV, agrees with the measurement (175.165 ± 0.050 eV) of Diehl *et al.* [Phys. Rev. A **56**, R1071 (1997)]. Apart from specifics, the paper discusses or points to certain basic aspects of computational quantum mechanics of such multiply excited states. For example, it refers to the utility of open-channel-like configurations toward proper convergence to a local energy minimum in the continuous spectrum, where quasibound and unbound states of the same symmetry lie below, and for which the normal eigenvalue properties of the discrete spectrum do not apply. Also, we discuss the possibility that is given by the state-specific theory for carrying out economic and physically transparent calculations and for deducing semiquantitative conclusions about the interplay between electronic structure, interference, and autoionization widths.

DOI: 10.1103/PhysRevA.67.052501 PACS number(s): 31.25.Jf, 32.80.Dz

I. INTRODUCTION

Accumulated knowledge from *ab initio* calculations and from measurements indicates that excited states with multiple excitations of valence electrons to higher subshells can be formed in negative, neutral, and positive ions. Because of the change in nuclear attraction along an isoelectronic series, the spectral properties, the types of configuration interaction, and the degree of difficulty in understanding quantitatively such states vary considerably, the positive-ion part being easier to handle, in general, theoretically.

As regards the issue of electron correlation, which is best described in terms of one, two, three, etc., excitations from a zero-order space of bound functions into virtual space of closed and of open channels, aspects of it in connection to multiply excited autoionizing (resonance) states have been the object of study and analysis within the framework of a state-specific theory (SST) since the early 1970s, with exemplars the triply excited states (TESs) of three-electron atoms (He^-,Li,Be^+,…) in the $n=2$ shell, e.g., Ref. [1]. In short, the weakness of nuclear binding and a variety of interelectronic interactions and of near degeneracies, the existence of the underlying continuous spectrum and of other quasibound states of the same symmetry with lower energy, the proximity to thresholds and to other resonances, and the easy polarization of the neutral core, render the theory and computation of the localized part, Ψ_0, and of the energies and widths of resonance states of negative ions a rather intriguing many-body problem. This problem becomes more complex as one goes higher in energy and the density of states as well the number of open channels increase.

In this paper, we focus on intrashell TESs where the main shell is $n=3$. Results on such states based on *ab initio* calculation or on assumptions of models were published recently [2–4]. The main motivation for our work [2] was the identification of the peaks that had been measured in electron-He scattering experiments in the energy region of the $n=3$ doubly excited states (DESs) of He [5]. Once these results were made known, additional information was produced by Chung [3], who computed partial and total widths as well, by diagonalizing complex matrices and obtaining complex eigenvalues in a two-step methodology. (See Refs. [1,6] for the background and justification of this methodology.) Also, Morishita and Lin [4] presented a semiquantitative analysis of angular correlation, based on a model where the three electrons are confined on the surface of a sphere [7]. Such a model draws some validity from the *ab initio* treatment of specific TESs that was published in Ref. [8], where numerical results and analysis showed the tendency of electron density to form an equilateral triangle, as energy increases towards the three-electron ionization threshold.

In addition to $n=3$ TESs of He^-, we calculated the relative positions of the $3s^2 3p\ ^2P^o$ and $3s3p^2\ ^4P$ intrashell TESs along the isoelectronic sequence, in order to make the connection with arguments concerning the spectrum of He^-. Calculations on these states in N^{4+} have been published in Ref. [9], from which the energy difference between the $^2P^o$ and ^4P states was predicted.

*Email address: npiang@eie.gr
†Email address: can@eie.gr

The sections that follow start with the presentation of the relevant published results and their significance. Section III comments briefly on certain characteristics of the theoretical framework in which these calculations were carried out. Section IV discusses the choice, the calculation, and the nature of the wave functions of the He DESs that were used as thresholds. Section V discusses the calculation and results for the energies and widths of the He^- TESs. Comparison is made with the calculations of Ref. [3] and with the experimental values of Ref. [5]. Section VI discusses basic features of the state-specific calculations and their application to the determination of the $E(^4P)-E(^2P^o)$ separation along the isoelectronic sequence. Given the fact that there have been recent measurements and calculations for the position of the Li $^2P^o$ state, we test the level of accuracy and consistency of our method by comparing with them. Section VII comments on the significance of the *open-channel-like* (OCL) configurations that enter in the multiconfigurational Hartree-Fock (MCHF) computation of the zero-order wave functions of multiply excited states. The presence of the OCL configurations results in the avoidance of possible ''sinking'' of the variationally obtained energy (which is a local minimum inside the continuous spectrum) and secures good convergence for the MCHF calculation. Finally, Sec. VIII discusses aspects of the interplay between the state-specific electronic structure of initial and final states in an autoionizing transition and the semiquantitative characteristics of decay dynamics, with application to the partial widths of the He^- TESs.

II. RESULTS ON THE LOWEST THREE $n=3$ INTRASHELL TESs OF He^-,Li,...,N^{4+} HAVING THE $^2P^o$, ^4P, AND ^2D SYMMETRIES

The work published in Ref. [2] predicted the existence of 11 He^- TESs in the energy region of the DESs of He in the $n=3$ shell, which can in principle be excited in collisions of electron colliding with He in the $1s^2\ ^1S$ or $1s2s\ ^3S$ states [2]. The $^2P^o$ (at 68.8 eV) and ''$3s3p^2$'' ^2D (at 69.1 eV) TESs of He^- were shown to correspond to the 1,1′ features of the scattering spectrum measured at 68.83 ± 0.04 eV and 69.00 ± 0.04 eV by Roy [5]. The ^4P state cannot be excited in an electron-scattering experiment from the $1s^2\ ^1S$ or the $1s2s\ ^3S$ discrete states of He, and so it was not computed. This state was subsequently computed by Chung [3]. One of his main conclusions, as recorded in the abstract of Ref. [3], is that: ''*...the spectrum (of the* $n=3$ *TES) is very different from that of the* He^- $2\ell 2\ell' 2\ell''$ *states. A* $3s$-$3p$ *energy inversion is uncovered*.'' By inversion it is meant that, in the $n=3$ shell, the $3s3p^2\ ^4P$ state is, according to Ref. [3], below the $3s^23p\ ^2P^o$ state by 7 meV. In other words, the filling of the subshells in the lowest states of the $n=3$ shell as a function of energy seems to be abnormal. On the contrary, in the $n=2$ shell the energy of the $2s2p^2\ ^4P$ state is above that of the $2s^22p\ ^2P^o$ state. As we will discuss below, our calculations and analysis indicate that no such inversion exists.

In fact, regarding this ''inversion'' for the $^2P^o$ and ^4P TESs, it was first predicted to exist in the ionized N^{4+} by Vaeck and Hansen [9], who carried out configuration interaction calculations for a large number of $n=3$ TESs which lie in the continuous spectrum. They predicted that the ^4P state is about 40 meV below the $^2P^o$ one. However, the level of sophistication and of accuracy of these calculations is not sufficiently high. For example, Bachau [10] computed the energy of the $^2P^o$ state as -7.0338 a.u., whereas the one given in Ref. [9] is -7.0897 a.u., i.e., 1.52 eV below. [This is a case of variational collapse (or ''sinking'') and not of a better energy.] Our state-specific calculations show that there is no inversion in N^{4+} either. Here, the $n=3$ ^4P intrashell TES is above the $^2P^o$ one by 59 meV, and the $n=2$ ^4P intrashell TES is above the $^2P^o$ one by about 430 meV.

In order to calibrate our He^- results, we also computed the $^2P^o$ and ^4P $n=3$ TESs in Li. For the $^2P^o$ state, there have been recent measurements as well as calculations [11,12]. We will compare our results with the ones of Refs. [11,12] in Sec. VI.

Finally, there is the question of the widths of the three TESs in He^-. The first such results were presented by Chung [3]. He produced partial widths in the independent channel approximation (ICA), as well as total widths. The calculations of Ref. [3] followed a two-step methodology with real and complex basis sets, whereby in the first step the calculation is done with only real functions on the real energy axis and obtains a localized wave function and a real energy, and in the second step a suitable set of complex functions is added and diagonalization of the non-Hermitian matrix yields the complex eigenvalues of the resonance states [6]. The present work has produced partial and total widths using real bound and scattering functions, and energy-dependent ''golden rule'' type formulas. These are compared in Table II to the results of Ref. [3].

III. BRIEF REVIEW OF THEORETICAL ASPECTS

The justification and the basics of the computational methodology that we employed in this work have been described in Refs. [1,2] and in their references. The SST calculations on TESs have shown that these states are optimally described in zero order by a MCHF wave function with suitably chosen configurations, under conditions that secure orthogonality to lower states. Such an orthogonality is necessary since the autoionizing (resonance) states are inside the continuous spectrum, and the energy of their localized part can only be a local minimum. This implies that during an optimization with respect to energy of a wave function with initially bound-state features, the solution may either collapse toward the energy of the $(N-1)$ electron threshold plus a zero-energy free electron, or may simply sink improperly to an energy that is slightly lower than the accurate local minimum.

Valid MCHF solutions for such strongly mixed wave functions are often hard to obtain, needing computational experience as well as attention through the prism of electronic structure theory and of numerical analysis. Either during the determination of the MCHF solution or, subsequently, during the variational calculation on the full Ψ_0 and E_0, a significant parameter for the proper convergence to the TES of interest is the type and extent of orthogonalization to lower states. Orthogonalization of occupied (MCHF) or of

virtual orbitals to orbitals of states of lower energy, including the $(N-1)$ or $(N-2)$ channel states, affects the degree of satisfaction of the virial theorem, which has been used by us as a fundamental index of localization. However they are introduced, orthogonality and optimization of the appropriate function spaces should be done while ascertaining that the virial theorem is satisfied to a very good degree.

Since the theory focuses on the state-specific quasibound N-body problem directly, it does not have to explicitly differentiate between ''Feshbach'' and ''shape'' resonances when computing the localized part Ψ_0. This distinction has been part of the scattering formalism for the formal treatment of resonance states. As we have argued before, Refs. [1,2], regarding the aim of determining the existence and identification of a multiply excited resonance the important criterion is whether the solution is localized in a reliable local minimum in the continuous spectrum, regardless of whether its position is above or below a nearby DES of the $(N-1)$-electron system. The question of whether this position is above or below a particular nearby threshold acquires importance when one pursues the calculation of the partial and total scattering cross sections or of the partial and total decay widths, so as to be able to distinguish the open channels.

Finally, we stress the significance of what we have called the OCL configurations, in the solution of the many-body problem. Ψ_0 is a polyelectronic wave packet whose construction follows guidelines of the theory of electronic structure. It consists of components representing the closed channels, but it may also contain contributions from bound configurations having the configurational structure of the adjacent continuous spectrum, as long as they do not destroy its localization, Refs. [1,2]. We have argued that the self-consistent incorporation of certain OCL configurations expedite convergence to the accurate position of the resonance. In most cases of symmetry and electronic structure, their inclusion in a MCHF calculation is feasible, and their energies may lie above or below the resonance of interest. However, there are cases where convergence of the MCHF calculation is not possible when a particular OCL is included. For example, this happens with the He^- $2s2p^2\ ^2S$ structure, with the open channel being $(He''2s^{2''})\varepsilon s\ ^2S$. Here, valid convergence of the MCHF equations has not been achieved by us if the $2s^2\overline{s}$ configuration is included, where $\overline{s}$ is supposed to be a bound orbital. In such cases, the energy contribution from the interaction between the bound and the scattering components of the open channels (the energy shift Δ) must be computed completely from a second step, using two different types of function spaces. The first is in general multidimensional, representing Ψ_0 and possibly other square integrable wave functions of other resonances coupled to it. The second represents the continuous spectrum, either in terms of real scattering functions (or L^2 approximations to them) or in terms of L^2 complex functions.

IV. THRESHOLDS AND He DOUBLY EXCITED STATES

It is clear from the zero-order structure of the He^- TES that these are embedded in an infinity of thresholds corresponding to states of He^+ and of He. For the calculation of off-diagonal bound-scattering matrix elements the most important channels are those created by the intershell DESs of He, where $n_1=2$ and $n_2=3$, since the corresponding matrix elements involve two active electrons. Since state-specific calculations produce accurate wave functions for such He DESs with only a few configurations (Table I), it is easy to see that the most significant decay channels to intershell DESs of He are those where the spin and the orbital angular momentum of the two active electrons do not change.

Table I presents the relevant results for all the He DESs that were used as thresholds in the numerical computation of fixed core scattering orbitals and in the subsequent calculation of the energy shifts and widths. It includes the computed energies and main mixing coefficients, the total size of the expansion, and the energies produced by other calculations [3,13], whose basis set expansions are orders of magnitude larger than the ones we used. As with all calculations on many-electron systems, especially for excited states, it is evident that the efficiency of the state-specific wave functions and energies is very high. Obviously, our aim was not to reach the limits of numerical accuracy. Rather, it was to combine compactness and electronic structure transparency with accuracy that is sufficient for the calculation of the above quantities. One of the significant points is that when the near-degeneracies and correlations are such that more than one- to three terms are needed for a good description, the total expansion is again very short.

For example, let us focus on the He DESs of $^3P^o$ and $^1P^o$ symmetries for which there is strong configurational mixing. The lowest state, corresponding to the main configuration $2s2p$, is excluded from the list since it corresponds to a change of three orbitals from the TESs of the $n=3$ shell. Numerical solution of the MCHF equations [14] shows that the next three $^3P^o$ and $^1P^o$ DESs are characterized by the heavy mixing [15] of the $2s3p$, $2p3s$, and $2p3d$ configurations. We obtained

$$|^3P^o(2)\rangle = 0.846\varphi(2s3p) + 0.425\varphi(2p3s) - 0.307\varphi(2p3d) \quad [\equiv \varphi(23sp_+)\ ^3P^o],$$

$$|^3P^o(3)\rangle = 0.780\varphi(2p3s) - 0.433\varphi(2s3p) - 0.452\varphi(2p3d) \quad [\equiv \varphi(23sp_-)\ ^3P^o],$$

$$|^3P^o(4)\rangle = 0.785\varphi(2p3d) - 0.548\varphi(2s3p) + 0.282\varphi(2p3s),$$

$$|^1P^o(2)\rangle = -0.690\varphi(2p3s) + 0.682\varphi(2s3p) - 0.242\varphi(2p3d) \quad [\equiv \varphi(23sp_-)\ ^1P^o],$$

$$|^1P^o(3)\rangle = 0.754\varphi(2s3p) + 0.663\varphi(2p3s) + 0.043\varphi(2p3d) \quad [\equiv \varphi(23sp_+)\ ^1P^o],$$

$$|^1P^o(4)\rangle = 0.808\varphi(2p3d) - 0.537\varphi(2s3p) - 0.233\varphi(2p3s).$$

TABLE I. Intershell doubly excited states of He used as thresholds for the calculation of widths of the He^- $n=3$ triply excited states. N, number of symmetry-adapted MCHF configurations in the approximate Ψ_0. The energies (in a.u.), are compared with those of Refs. [3,13]. The third column lists the main configurations and their mixing coefficients.

State	N	This work Main configurations	E (a.u.)	Ref. [3] E (a.u.)	Ref. [13] E (a.u.)
$^1S(3)$	3	$2s3s(0.789)$, $2p3p(0.596)$	−0.589 16	−0.589 955	−0.589 89
$^1S(4)$	5	$2p3p(-0.832)$, $2s3s(0.478)$	−0.543 44	−0.548 127	−0.548 09
$^3S(1)$	2	$2s3s(0.810)$, $2p3p(0.586)$	−0.602 43	−0.602 578	−0.602 58
$^3S(2)$	2	$2p3p(-0.786)$, $2s3s(0.618)$	−0.558 37	−0.559 747	−0.559 75
$^1P(1)$[a]	1	$2p3p$	−0.579 41	−0.580 245	−0.580 25
$^3P(2)$[a]	2	$2p3p(0.984)$, $2p^2(0.179)$	−0.566 33	−0.567 799	−0.567 81
$^1D(2)$	3	$2p3p(0.874)$, $2s3d(-0.442)$	−0.566 60	−0.569 210	−0.569 22
$^1D(3)$	3	$2s3d(0.891)$, $2p3p(0.452)$	−0.549 90	−0.556 392	−0.556 42
$^3D(1)$	2	$2p3p(-0.885)$, $2s3d(0.466)$	−0.582 74	−0.583 784	−0.583 78
$^3D(2)$	2	$2s3d(0.870)$, $2p3p(0.493)$	−0.554 01	−0.560 611	−0.560 69
$^1P^o(2)$	14	$2p3s(-0.690)$, $2s3p(0.682)$, $2p3d(-0.242)$	−0.597 07	−0.596 640	−0.597 07
$^1P^o(3)$	11	$2s3p(0.754)$, $2p3s(0.663)$, $2p3d(0.043)$	−0.564 10	−0.563 921	−0.564 09
$^1P^o(4)$	14	$2p3d(0.836)$, $2s3p(-0.504)$, $2p3s(-0.215)$	−0.546 99	−0.547 093	−0.547 10
$^3P^o(2)$	14	$2s3p(0.846)$, $2p3s(0.425)$, $2p3d(-0.307)$	−0.584 57	−0.584 812	−0.584 67
$^3P^o(3)$	14	$2p3s(0.780)$, $2p3d(-0.451)$, $2s3p(-0.433)$	−0.578 85	−0.579 012	−0.579 03
$^3P^o(4)$	14	$2p3d(0.785)$, $2s3p(-0.548)$, $2p3s(0.282)$	−0.548 62	−0.548 832	−0.548 81
$^1D^o(1)$[a]	1	$2p3d$	−0.562 24	−0.563 792	−0.563 80
$^3D^o(1)$[a]	1	$2p3d$	−0.558 29	−0.559 310	−0.559 33
$^1F^o(1)$	1	$2p3d$	−0.553 05	−0.558 275	−0.558 28
$^3F^o(1)$	1	$2p3d$	−0.560 26	−0.566 212	−0.566 20

[a]Due to symmetry and parity these are discrete states.

By augmenting these wave functions to only a 14-configuration MCHF expansion, we obtained energies for these rather difficult cases that are in very good agreement with those from other types of calculations with very large expansions [3,13] (Table I). The reason for pursuing good accuracy for these wave functions is that, as we shall see, the lowest $^3P^o$ channel dominates the decay of the He^- $^2P^o$ state (together with the $2s3s$ ^3S channel), as well as of the ^4P and ^2D states. Furthermore, the transparency provided by the compact expansion allows the understanding of the contribution of various effects to all transition processes involving these DESs either as initial or as final states. In other words, as it was pointed out in the early 1980s [16,17], the possibility of computing state-specific MCHF solutions such as the ones above, allows the analysis and understanding of the interplay between electronic structure and excitation and decay properties, since it is relatively easy to recognize the main contributions and possible constructive or destructive interference. This will be further discussed in Sec. VIII, Table III, with an example.

V. CALCULATION OF THE He^- $n=3$ INTRASHELL TESs AND RESULTS

The applications involved the treatment of the $3s3p^2$ ^4P state and the computation of the energy shifts and widths for the $^2P^o$, ^4P, and ^2D $n=3$ intrashell TESs of He^-. The Ψ_0 and E_0 of $^2P^o$ and ^2D were taken from Ref. [2]. We start with the calculation of Ψ_0 and E_0 for the ^4P TESs of He^-.

Following the methodology that is presented in our previous work, we first obtained a 22-term MHCF solution with $E(22)_{\mathrm{MCHF}}=-0.373\,978\,4$ a.u.; virial, 1.997. The main contributions come from the following configurations (given with the corresponding mixing coefficients): $c(3s3p^2)=0.922$, $c(3s3d^2)=0.237$, $c(3d3p^2)=0.236$, $c(2s3p^2)=0.131$, $c(2p3s3p)=0.087$, $c(3s4p^2)=-0.062$, $c(3d^3)=0.060$. Explicit orthogonality to the He^+ $1s$ orbital was kept during optimization. Orthogonality to the most important lower multiply excited states is assured through the inclusion of OCL configurations containing the $2s$ and $2p$ self-consistent orbitals, such as the $2s3p^2$ or $2p3s3p$. It is an immediate result of this type of calculation that the three main orbitals, the $3s$, $3p$, and $3d$, are seen to occupy the same region, since their average radii are $\langle r\rangle_{3s}=8.98$ a.u., $\langle r\rangle_{3p}=8.27$ a.u., $\langle r\rangle_{3d}=8.34$ a.u.

It is worth noting that by careful optimization and analysis, legitimate higher lying He^- ^4P localized states can also be established using this wave function. However, this is not the purpose of this paper.

Using the 22-term MCHF localized solution, we proceeded with the final configuration-interaction calculation using variationally optimized virtual orbitals with orbital angular momentum up to $\ell=7$ and symmetry-adapted configurations with one-, two-, and three-electron excitations. The energy of a 193-term expansion is $E_0=-0.374\,708\,9$ a.u. The next root is 1435 meV above, and does not influence the final result.

TABLE II. Calculated partial and total decay widths (in meV) for the $3s^2 3p\ ^2P^o$, $3s3p^2\ ^4P$, and $3s3p^2\ ^2D$ He^- resonance states. 1 a.u. (He) = 27.2077 eV.

		γ_i (meV)							
Channel		$^2P^o$		^4P			^2D		
Threshold	εl	This work	Ref. [3]	εl	This work	Ref. [3]	εl	This work	Ref. [3]
$2s3s\ (^1S)$	εp	68.5	54.5				εd	0.02	4.9
$2p3p\ (^1S)$	εp	3.9	0.4						
$2s3s\ (^3S)$	εp	4.1	2.9				εd	0.04	
$2p3p\ (^3P)$	εp	2.6	7.8	εs	1.8		εd		
				εd	31.8	32.1			2.0
$2p3p\ (^1D)$	εp	1.3	3.6				εs	35.6	31.0
$2s3d\ (^1D)$	εp		0.5				εs	3.1	2.7
$2p3p\ (^3D)$	εp	8.0	8.8	εd	0.6	0.6	εs	13.9	11.5
$2s3d\ (^3D)$	εp	1.5	1.7	εd	3.1	2.2	εs	6.9	3.1
$23sp_+(^3P^o)$	εs	61.3							
	εd	2.5	76.1	εp	130.8	116.8	εp	62.2	99.1
							εf	45.3	
$23sp_-(^3P^o)$	εs	4.1	0.8	εp	1.5	0.5	εp	2.2	
							εf	0.06	1.4
$2p3d\ (^3P^o)$	εs	0.02		εp	0.7	0.3	εp	1.2	
$23sp_-(^1P^o)$	εs	4.5	4.1				εp	0.4	
$23sp_+(^1P^o)$	εs	8.3	10.6				εp	7.0	13.5
$2p3d\ (^1P^o)$	εs	0.05					εp	0.02	
$2p3d\ (^3D^o)$				εp	1.1	1.3	εp		3.7
$2p3d\ (^3F^o)$							εp		1.7
Total		171	176		171	156		178	177

The calculation of the total energy shift Δ, partial widths γ_i, and total width Γ

In our previous calculation of the $^2P^o$ and ^2D TESs [2], the calculation of the shifts due to the explicit consideration of scattering orbitals for the open channels was not done. This is because the self-consistent inclusion of the OCL configurations produced energies of sufficient accuracy so as to explain the measurements of Roy [5]. Only for the ''$3s3p^2$'' ^2S state was the calculation less accurate, since the OCL configuration $3s^2\overline{s}\,^2S$ was not included, due to uncertainties in the proper convergence of the MCHF solution. Therefore, its contribution should have been included via the use of scattering functions and the corresponding interaction with the Ψ_0, something which was outside the goal of Ref. [2]. Anyway, the approximate position of this state shows that it is not needed for the interpretation of the measurements [5].

The procedure and the formulas for the calculation of Δ, the partial widths γ_i, in the ICA and the total width Γ, have been justified in our previous publications. They involve the iterative solution of the transcendental equation

$$\mathcal{E}-E_0-\delta_i(\mathcal{E})=0 \tag{1a}$$

with the partial energy shift given by

$$\delta_i(\varepsilon)=\mathrm{P}\int_{E_i}\frac{|\langle\Psi_0|H-\mathcal{E}|U_i(\varepsilon)\rangle|^2}{\mathcal{E}-\varepsilon}d\varepsilon. \tag{1b}$$

The $U_i(\varepsilon)$ wave functions are the N-electron fixed core scattering functions, not necessarily orthogonal to Ψ_0.

The total energy is obtained by adding to E_0 the sum of the partial shifts,

$$E=E_0+\Delta=E_0+\sum_i\ \delta_i\,. \tag{2}$$

Once the position of the resonance is determined, the partial widths are computed from

$$\gamma_i(E)=\frac{2\pi|\langle\Psi_0|H-E|U_i(E)\rangle|^2}{1-\delta_i'(E)}, \tag{3}$$

where $\delta_i'(E)$ is the derivative of the energy shift at the position of the resonance state E. Its size signifies the degree of energy dependence of the width. For narrow resonances, $\delta_i'(E)$ is negligible and so the standard golden rule result is recovered.

The results are shown in Table II. The partial energy shifts and widths are computed in the ICA, and no interchannel coupling is accounted for. Therefore, although there is good understanding of the factors that contribute to each channel separately, there is still uncertainty as to the effect of interchannel coupling on each partial width. However, such coupling is expected to have a small effect on the total width, since it essentially causes a redistribution (small or large,

depending on the system and the channel) of the partial widths [18]. The Δ and Γ are obtained as sums of the partial shifts and widths.

The final results for the nonrelativistic total energies are [1 a.u. (He) = 27.2077 eV, E(He) = −2.903 724 a.u.]:

$$E(^2P^o) = E_0 + \Delta = -0.375\,855\,1 \text{ a.u.} + 0.000\,523 \text{ a.u.}$$
$$= -0.375\,332\,4 \text{ a.u.}$$
$$= 68.79 \text{ eV above the He } 1s^2 \text{ state,}$$

$$E(^4P) = E_0 + \Delta = -0.374\,708\,9 \text{ a.u.} + 0.000\,458 \text{ a.u.}$$
$$= -0.374\,250\,9 \text{ a.u.}$$
$$= 68.82 \text{ eV above the He } 1s^2 \text{ state,}$$

$$E(^2D) = E_0 + \Delta = -0.365\,546\,2 \text{ a.u.} + 0.002\,075 \text{ a.u.}$$
$$= -0.363\,471\,2 \text{ a.u.}$$
$$= 69.11 \text{ eV above the He } 1s^2 \text{ state.}$$

The small difference between the energies of the $^2P^o$ and ^4P states, in conjunction with the widths of Table II, shows that the two resonances overlap. Of course, in an electron-He scattering experiment such as the one of Ref. [5], the ^4P state is not excited.

It is noteworthy that the shift in the energy of the ^2D state from its E_0 value is due mainly to the $23sp_+$ $(^3P^o)\varepsilon f$ channel, which adds 45 meV, out of the total of 56 meV. This is caused from the direct interaction with the $3s3p^2$ configuration, where the two-electron matrix element for the deexcitation $3p^2 \rightarrow 2p\varepsilon f$ is large. The MCHF calculation did not include a bound OCL configuration of the type $(23sp_+)f$. However, it did include OCL configurations such as $2s3s3d$, corresponding to the replacement $3p^2 \rightarrow 2s3d$. This OCL configuration does not contribute much to energy but it does contribute to proper orthogonality to lower states and therefore to proper convergence. On the contrary, the intrashell replacement, $3p^2 \rightarrow 3s3d$ is, as expected, significant, yielding a coefficient for the corresponding $3s^23d$ configuration of 0.45.

Roy's measurements [5] produced a peak (structure 1 of his spectrum) at 68.83 ± 0.04 eV and a second peak (structure 1′) at 69.00 ± 0.04 eV. These two peaks seem to overlap, and the total width given by Roy for the (1-1′) structure is 180 ± 40 meV. Our values for the total widths of the $^2P^o$ and ^2D TESs are 171 and 178 meV, respectively. Those of Chung [3] are 176 and 177 meV.

VI. THE $E(^4P) - E(^2P^o)$ SEPARATION ALONG THE ISOELECTRONIC SEQUENCE

The calculated energies in Ref. [3] for the three TESs of interest are, $^2P^o$, 68.75 eV; ^4P, 68.74 eV, and ^2D, 68.94 eV. These numbers indicate that the $^2P^o$ state is higher than the ^4P state, albeit by a very small difference, contrary to the spectrum of the $n=2$ intrashell TESs, where the $^2P^o$ state is lower by about 200 meV. Since this "inversion" is not corroborated by our calculations, below we examine the issue more systematically.

The immediate observation is that our numbers are a bit higher than those of Ref. [3]. By comparing with the experimental values of Roy [5], we see that for the $^2P^o$ state our result is within the error margin of his 68.83 ± 0.04 eV. For the ^2D state, both calculations have yielded energies that are slightly outside the error margin of the measured one (69.00 ± 0.04 eV). Ours is higher by 0.11 eV and that of Chung [3] is lower by 0.16 eV.

As we have argued in the framework of the SST, for many-body systems such as the multiply excited states, the problem of solving the effective matrix eigenvalue equation for the localized Ψ_0 has three major components. The first is the possibility of accounting for the self-consistent field and the long-range interactions created by the few main configurations. The relaxation that occurs in subshells that are excited and of large extent cannot be represented efficiently by fixed basis sets. The second component of the SST is the possibility of incorporating the details of the remaining localized electron correlation. The third is to carry out the multielectron calculation and to reach convergence to the correct local minimum inside the continuous spectrum by excluding the function space (due to open channels and to lower quasibound states) that may cause small or large "sinking" of the solution for the energy.

In the paragraphs below, we will discuss our calculations in terms of these three components. As regards the difference with the results of Ref. [3], we think that it has to do with the way orthogonality to lower states is accounted for. The calculations of Ref. [3] are supposed to optimize a multiparameter function space using orbital orthogonality constraints and the mini-max theorem, see the discussions in Refs. [6,19,20]. However, the level of precision of such multiparameter optimization procedures in the continuous spectrum is not clear-cut. Since no information on this part of the calculation is given in Ref. [3], we cannot reach a definitive conclusion as to why the energies of the three TESs computed by Chung [3] are slightly lower than ours.

We start the study with results from Hartree-Fock (HF) calculations. We found $E_{\rm HF}(^4P) = -0.364\,858\,7$ a.u., obtained with the $3s$ orbital being kept orthogonal to the He^+ $1s$ and $2s$ orbitals, and the $3p$ orbital being kept orthogonal to the He^+ $2p$ orbital [1,6]. The virial is 2.16. For the $^2P^o$ state, $E_{\rm HF}(^2P^o) = -0.337\,249\,5$ a.u., i.e., about 750-meV higher, and the virial is 2.13. It is clear that extra orbital orthogonality, which is implemented via the addition of Lagrange multipliers in the HF equations, reduces the accuracy of the virial. It is stressed that the satisfaction of the virial theorem (an index of localization) is an intrinsic property of the HF equations, as long as there are no extra Lagrange multipliers. For example, if we take the orbitals from the previous solutions and optimize carefully without the extra orthogonalities, the localized solutions are still obtained in the same "wells" [1], with energies $E_{\rm HF}(^4P) = -0.362\,671$ a.u. and $E_{\rm HF}(^2P^o) = -0.336\,226$ a.u. (the difference is now 719 meV), and with the virial being 2.0. These results show that the extra orbital orthogonalities may lead to a slight "sinking" of the energy of the local minimum, at the

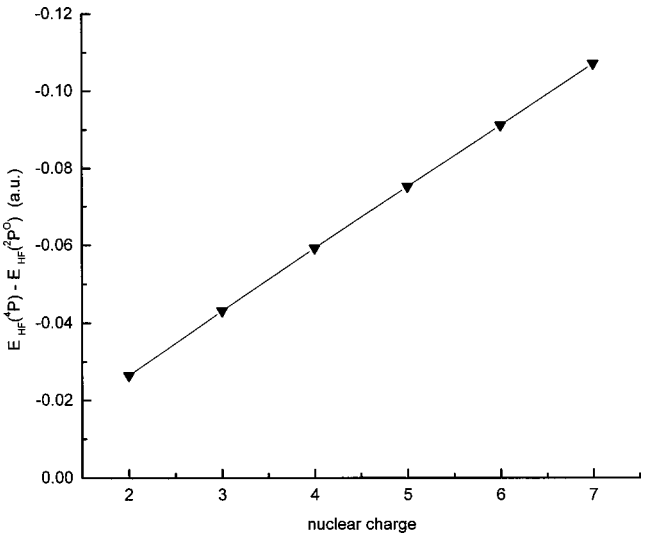

FIG. 1. Difference of the Hartree-Fock energies, in a.u., of the $3s^2 3p\ ^2P^o$ and $3s3p^2\ ^4P$ states, for $Z=2,3,...,7$.

expense of the precise satisfaction of the virial.

The fact that the HF energies put the ^4P TES below the $^2P^o$ one characterizes the whole isoelectronic sequence. Figure 1 shows the difference $E_{\mathrm{HF}}(^4P)-E_{\mathrm{HF}}(^2P^o)$, for He^- (719 meV), Li (1173 meV), Be^+ (1612 meV), B^{2+} (2047 meV), C^{3+} (2481 meV), and N^{4+} (2914 meV). The plot of $E_{\mathrm{HF}}(^4P)-E_{\mathrm{HF}}(^2P^o)$ versus Z is essentially linear. It follows that the inverted sequence of these states in their respective spectra (i.e., ^4P is above the $^2P^o$ state) is the result of the different sizes of localized electron correlation (mainly) and of the remaining interactions with open channels.

We now come to the inclusion of localized electron correlation, so as to obtain the full Ψ_0 and E_0 while examining the possible effects of orbital and state orthogonality.

Before any calculation is done, it is clear from the electronic structure of the states that there is more electron correlation in the $3s^2 3p\ ^2P^o$ state than in the $3s3p^2\ ^4P$, due mainly to the near-degeneracy mixing $3s^2 3p \leftrightarrow 3p^3$, which is absent from the ^4P symmetry. On the other hand, in both states the strongly mixing replacement $\ell \rightarrow \ell+2$, i.e., $3s \rightarrow 3d,4d,\ldots$. and the replacements of the pairs $(3s3p)$ and $3p^2$ should contribute significantly. (For the *a priori* identification and for the calculation of the important correlation effects in excited states of *N*-electron atoms, see the reviews of Ref. [21].) When we restrict the function space to the $n=3$ orbitals and carry out MCHF calculations, the expansion for the ^4P state contains four configurations and the one for the $^2P^o$ state contains seven. The solutions that are obtained by orthogonalizing the $n=3$ orbitals of He^- to the He^+ orbitals gave the following energies (without a very good virial): $E(4)_{\mathrm{MCHF}}(^4P)=-0.375\,691$ a.u., virial$=2.15$, and $E(7)_{\mathrm{MCHF}}(^2P^o)=-0.375\,627$ a.u., virial$=2.12$. The two states are essentially degenerate at this level of approximation. When the orthogonality constraint is lifted, again, as in the case of the HF solutions, the virial is satisfied exactly while the energies remain in the same wells, with only small changes upwards. Specifically, $E(4)_{\mathrm{MCHF}}(^4P)=-0.372\,846$ a.u., virial$=2.0$, and $E(7)_{\mathrm{MCHF}}(^2P^o)=-0.373\,832$ a.u., virial$=2.0$. Hence, at this level of approximation, the $^2P^o$ state is below the ^4P by 27 meV.

The same behavior of the roots is observed when the MCHF expansion is augmented. The approximate exclusion of lower states via orbital orthogonality to He^+ $1s$, $2s$, $2p$ orbitals reduces the level of satisfaction of the virial condition and at the same time produces slightly lower energies than the ones obtained when optimization of the MCHF solution is continued without these orthogonalities, in which case the virial is satisfied exactly. Thus, using a 17-term expansion for the ^4P state and a 33-term expansion for the $^2P^o$ state, the MCHF energies are: $E(33)_{\mathrm{MCHF}}(^2P^o)=-0.374\,715$ a.u. and $E(17)_{\mathrm{MCHF}}(^4P)=-0.373\,814$ a.u., the $^2P^o$ state being lower by 25 meV.

The alternative to multiple orbital orthogonalization is to include in a large MCHF calculation OCL configurations, whose structure is $2\ell 3\ell' 3\ell''$. Of these some represent true, lower lying resonance states, such as $2s3p^2\ ^4P$ or $2s3s3p\ ^2P^o$. Configurations with one or more orbitals with $n=1$ (e.g., $1s2s3p$) or with two orbitals in the $n=2$ shell (e.g., $2s2p3p$) are excluded, since they are coupled very weakly, their energy contribution is negligible and may not allow convergence to a proper MCHF solution.

The presence of OCL configurations facilitates convergence of the state-specific MCHF calculation while ensuring state orthogonality to reasonably accurate representations of lower states. Thus, we carried out two large MCHF calculations with the following characteristics. For the ^4P state we used 22 configurations, of which five were of the OCL type. The result is $E(22)_{\mathrm{MCHF}}(^4P)=-0.373\,978$ a.u. with the virial being 1.997. For the $^2P^o$ state we used 43 configurations, of which ten were of the OCL type. The result is $E(43)_{\mathrm{MCHF}}(^2P^o)=-0.375\,209$ a.u., with the virial being 2.001. These results show that by carrying out the MCHF optimization in the presence of the important OCL configurations, both the virial theorem and state orthogonality to the nearby important lower states (represented by OCL configurations) are satisfied.

Once the MCHF solutions are acceptable, the remaining localized electron correlation is included variationally, using virtual function spaces with one-, two-, and three-electron excitations. This approach to the calculation of localized electron correlation has been applied in a unified way within the SST, regardless of whether the state is excited or not, e.g., Refs. [1,2,6,21–24]. However, in the case of resonance states, i.e., of quasilocalized states in the continuous spectrum, the quantum mechanics of the many-electron calculation cannot rely on the energy-minimum variational principle that holds for the discrete spectrum. This is why we have given this discussion, here as well as in earlier publications.

We now comment on the level of numerical accuracy and reliability of the final results, since the $E(^4P)-E(^2P^o)$ separation that is being pursued is very small, of the order of 1×10^{-3} a.u.

There are three steps comprising the determination of the positions of these states and of their separation. The first one involves the MCHF calculation, with care concerning orthogonality to lower states and the satisfaction of the virial

theorem. Since the solution is numerical, errors from use of basis functions are absent. The second one involves the calculation of the remaining localized correlation. This is carried out variationally, by expanding systematically the function space of virtual orbitals and correlation configurations until convergence to the local energy minimum is satisfactory. For example, let us take the $^2P^o$ state. The 43-term MCHF energy is $-0.375\,209$ a.u. When 178 symmetry-adapted correlation configurations are added, i.e., when the total number of configurations is 221, E_0 is found to be $-0.375\,737\,7$ a.u. This localized wave function is constructed from the MCHF orbitals $2s$, $2p$, $3s$, $3p$, $3d$, $4s$, $4p$, $4d$, $4f$ and from optimized virtual orbitals, v_ℓ, with $\ell = 0,1,2,3,4,5$ and with one Slater-type orbital (STO) per orbital angular momentum. When another 360 configurations are added, we reach our final result, for a total of 581 configurations, of $E_0 = -0.375\,854\,7$ a.u. Now, the virtual space is constructed from STOs with $\ell = 0,1,2,3,4,5,6,7$. The orbitals of the singly excited configurations are nonorthogonal to those of the doubly excited ones. Selected triply excited configurations are also included. The convergence of such a calculation is at the level of 10^{-4} a.u., i.e., about 3 meV. A similar type of convergence is observed for the ^4P state. Obviously, when the difference of the energies of the ^4P and $^2P^o$ states is taken, the accuracy is at the level of 10^{-4} a.u. or better.

The third step involves the computation of the energy shift Δ, due to the interaction of Ψ_0 with the open channel scattering functions. In the present case, these quantities turn out to be very small, since part of the contribution of the continuous spectrum is taken into account by the OCL configurations during the computation of E_0 (Secs. III and VII). Even if the result for the Δ of each state were wrong by a factor of 2 in the wrong direction, the difference of the total energies would still show that the $^2P^o$ state is lower than the ^4P one by 9 meV.

Table III lists the results for the lowest $n=2$ and $n=3$ ^4P and $^2P^o$ TESs, including the contribution of the energy shift Δ. The table also contains results from other calculations. For the $n=3$ case, the last two columns compare the present results with those of Ref. [3]. The total energies that were obtained by the methodology of this work indicate that there is no inversion in the filling of the $n=3$ subshells and that the He^- $3s^2 3p\ ^2P^o$ state is 29 meV below the $3s3p^2\ ^4P$ state. Here we should note that a conclusion from our computations of the TESs of the $n=2$ and $n=3$ shell, is that for $n=2$ it is necessary to include configurations from the $n=3$ and $n=4$ shells before the energy difference starts stabilizing. On the other hand, for the $n=3$ TESs this convergence is apparent already at the stage where only the $n=3$ configurations are included in the MCHF calculation. This fact is in harmony with the results that were obtained in the 1980s regarding the DESs, and which showed that as n increases, the correlation of the intrashell states is essentially described by the MCHF intrashell configurations [22].

The Li atom and its isoelectronic sequence

Given the difference between our conclusions and those of Ref. [3] for the spectrum of He^-, and given the fact that, as we already mentioned in Sec. II, a prediction for ''inversion'' between the ^4P and $^2P^o$ states in the $n=3$ shell was published in Ref. [9] for the N^{4+} ion as well, we studied the issue of the calculation of TESs in Li and in the positive ions up to $Z=7$. It is natural to expect that for these systems convergence is less demanding than in He^-. We already gave in Fig. 1 and in Table III the HF energy difference, showing that, without correlation, the shell model predicts that the $3s3p^2\ ^4P$ state is below the $^2P^o$ one. As our results show below, the inclusion of the localized electron correlation restores the order, and the filling of the subshells starts with the $3s^2 3p\ ^2P^o$ state, which indeed is below the $3s3p^2\ ^4P$ TESs.

TABLE III. Values for the energy difference, in meV, between the $n=2$ and $n=3$ intrashell $ns^2np\ ^2P^o$ and $nsnp^2\ ^4P$ states of He^-, at various levels of approximation.

$\Delta E = E(^4P) - E(^2P^o)$ (meV)					
n	HF	MCHF$_n$[a]	MCHF$_{n,n+1}$[b]	FCI	FCI+Δ
2	-927.0	-171.5	-30.3[c]	204.3[d]	209.2[d]
			126.3[e]		207.0[f]
					210.0[g]
3	-719.6	27.1	33.5	31.3	29.4
	-751.2[h]	-1.8[h]	31.6[h]	-21.8[i]	-7.3[i]

[a]With configurations from orbitals of the n shell.
[b]With configurations from orbitals of the n and $n+1$ shells.
[c]Energy of $^2P^o$ from Ref. [1(a)] and energy of ^4P from a small (three-term) MCHF calculation [6].
[d]Energy of $^2P^o$ from Ref. [28] and energy of ^4P from Ref. [29].
[e]Energy of $^2P^o$ from Ref. [1(a)] and energy of ^4P from a larger (14-term) MCHF calculation [6].
[f]Reference [30].
[g]Energy of $^2P^o$ from Ref. [1(a)] and energy of ^4P from Ref. [30].
[h]With orthogonality to fixed He^+ $n=1,2$ orbitals, without OCL.
[i]Reference [3].

For Li, the calculations aimed at obtaining an accurate E_0 by using both steps of the state-specific methodology, i.e., first obtain a MCHF solution that includes OCL configurations and then add the remaining function space of the one-, two-, and three-electron virtual excitations for the localized correlation.

For the ions Be^+, B^{2+}, C^{3+}, and N^{4+}, convergence of the first step is efficient already at the MCHF level. Therefore, only the MCHF solutions with all configurations from the $n=3$ and $n=4$ shells, together with the OCL configurations, were used.

Specifically, for Li the MCHF wave function for the $3s^2 3p\ ^2P^o$ state consisted of 43 configurations, of which ten were of the OCL type $\{3s^2 2p, 2p3p^2(^3P, ^1D, ^1S), (2s3s)^1S, ^3S\ 3p, (2s3p)\ ^1P^o, ^3P^o 3d, (2p3s)^1P^o, ^3P^o 3d\}$. The corresponding energy is $-1.040\,181\,7$ a.u. The total Ψ_0 consisted of 581 symmetry-adapted configurations. The corresponding E_0 is $-1.040\,985\,6$ a.u. and the virial is 2.004. For the $3s3p^2\ ^4P$ state, the MCHF solution consisted of 22 configurations, of which five were of the OCL type $\{2s3p^2, 2s3d^2, 2p3s3p, 2p(3p3d)\ ^3P^o, ^3D^o\}$. The corresponding energy is $-1.038\,516\,4$ a.u. The total Ψ_0 consisted

of 193 configurations. The corresponding E_0 is $-1.039\,385\,9$ a.u. and the virial is 1.999. Since the difference $\Delta(^2P^o) - \Delta(^4P)$ is negligible, our prediction is that the ^4P state is above the $3s^2 3p\ ^2P^o$ state by 44 meV. (The difference of the MCHF energies gives 45 meV, i.e., the same result, showing that the remaining electron correlation is common for both states.)

It is significant here to compare with experimental values and with previous theoretical results that are available for the position of the Li $3s^2 3p\ ^2P^o$ state. These were published in 1997 by two groups of researchers [11,12]. The experiments involved the photoexcitation of this state using synchrotron radiation and photoion or photoelectron spectroscopy. Diehl *et al.* [11] measured the energy as 175.165 ± 0.050 eV above the ground state. Azuma *et al.* [12] measured it as 175.25 ± 0.10 eV. Our result is 175.15 eV, in very good agreement with the measurement of Ref. [11]. It is noteworthy that the predictions of large MCDF calculations are 174.11 eV [11] and 174.14 eV [12], a discrepancy from experiment of 1 eV. Large *R*-matrix computations in Ref. [11] produced 174.90 eV. The theoretical result closest to ours is that of Ref. [11], who diagonalized a large complex matrix with an eigenvalue corresponding to a position of 175.12 eV above the ground state. It is worth pointing out that, according to Ref. [11], the diagonalization of a 570-term real matrix with saddle point optimization [6,19,20] produced an energy of $-1.043\,414$ a.u., which is again, as in the case of He^-, lower (by 66 meV) than our value for E_0. As it was stated in Ref. [6] and in Sec. II of this paper, without detailed numerical evidence it is not clear how the multidimensional optimization via the mini-max theorem for eigenvalues has been implemented in Refs. [3,11], and how it secures a precise value for the real energy of a resonance state.

For the other ions, our calculations were carried out at the level of the MCHF wave functions and energies. For ions, when taking the difference of the energies of the two states, the result from the use of just the MCHF energies is reliable. Table IV contains the energy difference along the isoelectronic sequence for both the $n=2$ and the $n=3$ shells. For the $n=2$ states of $Z=5,7$, for which we avoided calculations for reasons of economy, we used interpolation and extrapolation. Comparison is made with published results that did not include the energy shift Δ. It is clear from these results that the difference increases with Z, toward a constant, nonrelativistic value. It is therefore necessary to discard the prediction of Vaeck and Hansen [9] for N^{4+}, where the ^4P state was placed above the $^2P^o$ state. We point out that the energy of our MCHF calculation for the $3s^2 3p\ ^2P^o$ state of N^{4+} (43 configurations) is $-7.030\,964$ a.u., in harmony with the large scale fixed basis calculations of Bachau [10], who also included OCL-type configurations with shell numbers (2,3,3) and found -7.0338 a.u.

Figure 2 depicts the difference between the energies of the four states, the $2s^2 2p\ ^2P^o$ and $2s2p^2\ ^4P$, and the $3s^2 3p\ ^2P^o$ and $3s3p^2\ ^4P$, for the sequence $Z=2-7$. It is true that this quantity becomes smaller in the $n=3$ shell, which is natural given the shrinking of the spectrum and the increase in the density of states. Nevertheless, our results still place the $^2P^o$ TES below the ^4P one. Of course, as n increases and the mixing becomes stronger, one must expect a variety of breakdowns of the predictions that may normally be made according to the single configuration model.

TABLE IV. Values of the energy difference, in a.u., between the $n=2$ and $n=3$ intrashell $ns^2np\ ^2P^o$ and $nsnp^2\ ^4P$ states for $Z=2,3,...,7$.

	$\Delta E = E(^4P) - E(^2P^o)$ (a.u.)	
Z	$n=2$	$n=3$
2	0.0077[a]	0.001 23,[b] 0.001 15,[c] −0.000 27[d]
3	0.0109[e]	0.001 67,[b] 0.001 60[c]
4	0.0128[f]	0.001 88[b]
5	0.0140[g]	0.002 01[b]
6	0.0149[f]	0.002 13[b]
7	0.0157[h]	0.002 17,[b] −0.001 47[i]

[a]Energy of $^2P^o$ from Ref. [28] and energy of ^4P from Ref. [29].
[b]State-specific MCHF energies, this work.
[c]Energy differences from FCI, state-specific calculations, this work.
[d]Reference [3].
[e]Reference [31].
[f]Reference [32].
[g]Interpolated value.
[h]Extrapolated value.
[i]Reference [9].

VII. COMMENTS ON THE OCL CONFIGURATIONS

We return to the calculation of the three lowest TESs of $n=3$ in He^- and we comment on the inclusion and the role of the OCL configurations at the level of the MCHF calculation. Let us focus on the ^4P state. The most important OCL configurations are the $2s3p^2$ [corresponding to the $(2s3p)\ ^3P^o\varepsilon p$ channel] and the $2p(3s3p)$ [corresponding

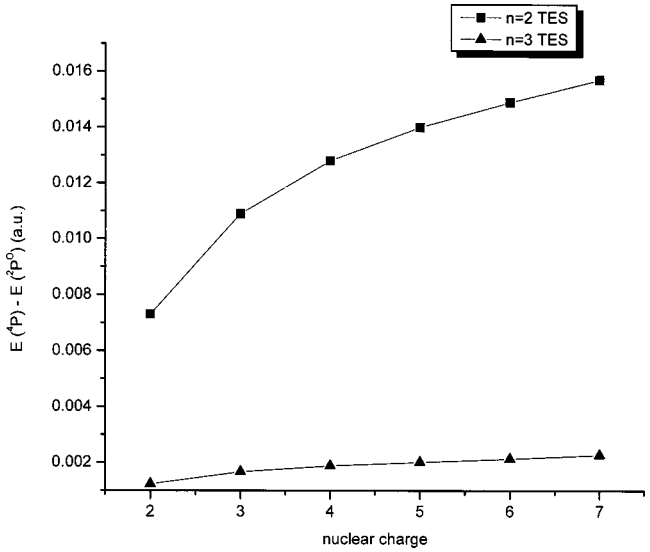

FIG. 2. Difference of the total energies, for the pairs of states $2s^2 2p\ ^2P^o$, $2s2p^2\ ^4P$ and $3s^2 3p\ ^2P^o$, $3s3p^2\ ^4P$, for $Z=2,3,...,7$. The text explains how and where these values were computed.

to the $(2p3s)\ ^3P^o\varepsilon p$ channel], with coefficients 0.1312 and 0.0871, respectively. Such coefficients are not negligible. In fact, as we shall see in the following section on widths, the channel $(2s3p)\ ^3P^o\varepsilon p$ draws the largest partial width, its value being 62 meV, while its contribution to the energy shift is only 5 meV. This is the result of the presence in the localized wave function of the OCL configuration. Analyses of such situations as regards the different effects of the OCL or Rydberg configurations due to their presence in the bound part of the off-diagonal interaction matrix element have been published in Refs. [1(b),23].

Similar conclusions are drawn for the partial widths and shifts in the $^2P^o$ and ^2D states. We have already mentioned the large partial energy shift (45 meV) for the $(2s3p)\ ^3P^o\varepsilon f$ channel of the ^2D TES, which appears because we did not include the corresponding OCL configuration (the MCHF calculation does not converge properly if the $(2s3p)\ ^3P^o4f\ ^2D$ configuration is included). On the other hand, if we consider the $2s3p^2\ ^2D$ MCHF OCL configuration, whose coefficient is 0.11, and which corresponds to the channel $\varphi(23sp_+)\ ^3P^o\varepsilon p$, we see that it causes the shift to be small, about 5 meV, while the partial width to this channel is large, about 62 meV. For the case of the $^2P^o$ state, let us consider the $(2s3s)\ ^1S\varepsilon p$ and $\varphi(23sp_+)\ ^3P^o\varepsilon s$ channels. Again, the partial energy shifts are very small (5 and 2 meV, correspondingly), because their contribution has been absorbed by the MCHF OCL configurations $(2s3s)^1S3p$, whose coefficient is 0.129, and $3s^22p$, whose coefficient is -0.043. However, the partial widths to these channels are large, being 68 meV for $(2s3s)\ ^1S\varepsilon p$ and 61 meV for $\varphi(23sp_+)\ ^3P^o\varepsilon s$ (Table II).

It is noteworthy that one of the problems of explicit orbital orthogonalities to lower orbitals of configurations of $(N-1)$ or $(N-2)$ for multiply N-electron states is the complication of the appearance of linear dependence of the basis sets. (For example, consider the case where different channels are created by singlet and triplet multiplicities for the same configurations.) On the contrary, such problems are eliminated if the major lower states to which we demand state orthogonality are represented explicitly via the MCHF OCL configurations. For example, let us consider the He $\varphi(23sp_+)\ ^3P^o$ and $\varphi(23sp_-)\ ^3P^o$ states of the $\varphi(23sp_+)\ ^3P^o\varepsilon s$ and $\varphi(23sp_-)\ ^3P^o\varepsilon s$ channels. If we take the orbital overlaps between the MCHF OCL orbitals of the $He^-\ ^2P^o$ TES and the orbitals of the He $^3P^o$ states, we see that this is large: $\langle(2s)_{\mathrm{He}}|(2s)_{\mathrm{He}^-}\rangle=0.9333$, $\langle(3s)_{\mathrm{He}^-}|(3s)_{\mathrm{He}^-}\rangle=0.9893$, $\langle(2p)_{\mathrm{He}}|(2p)_{\mathrm{He}^-}\rangle=0.9804$, and $\langle(3p)_{\mathrm{He}}|(3p)_{\mathrm{He}^-}\rangle=0.9679$. This orbital similarity makes the inclusion of the MCHF OCL configurations physically relevant.

VIII. RESULTS AND COMMENTS ON PARTIAL AND TOTAL WIDTHS

Table II contains our results for the partial and total widths of the three lowest TESs of He^-, the $3s^23p\ ^2P^o$, $3s3p^2\ ^4P$, and $3s3p^2\ ^2D$. The total widths are essentially the same for all three states. These are, $\Gamma(^2P^o)=171$ meV, $\Gamma(^4P)=171$ meV, $\Gamma(^2D)=178$ meV. For all of them, the dominant decay channel is the He $\varphi(23sp_+)\ ^3P^o$. In the case of $^2P^o$, there is also another dominant channel, the $\varphi(2s3s)\ ^1S$, whose width, 68 meV, is essentially the same as that of the $\varphi(23sp_+)\ ^3P^o$ channel (64 meV).

Table II also includes the results of Chung [3]. In both sets of calculations, the partial widths were obtained in the ICA. Considering the complexity of the problem, as regards the gross picture the agreement is very good, especially for the total widths. Differences appear for certain widths that are small. For example, for the $(2p3p)\ ^1S\varepsilon p$ channel of $^2P^o$, our value is 4 meV and that of Ref. [3] is 0.4. Or, for the $(2s3s)\ ^1S\varepsilon d$ channel in ^2D, our calculations indicate essentially no decay (0.02 meV) and those of Ref. [3] a small width of 5 meV.

The fact that the present approach employs state-specific compact wave functions where the main configurations contain recognizable and physically relevant orbitals, offers the possibility of understanding heuristically, in many cases, the interplay between electronic structure characteristics of the TESs and the computed partial widths. In fact, notions such as the ones outlined below, most often provide efficient understanding for phenomena such as two-electron excitations, collective excitations, localized transfer of transition strength, dominant electron correlations and absorption or decay spectra, the significance of internal couplings and overlaps in autoionization widths, etc.

The basics for this type of analysis have been presented in earlier work on state-specific many-electron treatments of photoabsorption or autoionization [17,21,24,25]. Two notions that are relevant here are as follows.

(1) The use and understanding of N-electron transition-matrix elements by reducing them to one- and two-electron interaction integrals, multiplied by overlap integrals that often contain much physical significance. For example, recent discussions and applications to TESs of Li and He^- of ideas where the calculation of orbital overlap leads to physically significant information, can be found in Refs. [26,27], where references to older work are also given.

In the present work, this notion can be used to interpret the difference in magnitudes of partial widths in the $n=2$, $2s^22p\ ^2P^o$ and $n=3$, $3s^23p\ ^2P^o$ states of He^-. These states decay preferentially to the He $\varphi(1s2p)\ ^3P^o$, $\varphi(1s2s)\ ^1S$ channels for the $n=2\ He^-$ TESs and to the $\varphi(23sp_+)\ ^3P^o$ and $\varphi(2s3s)\ ^1S$ channels for the $n=3$ TESs. By writing the decay matrix elements, it becomes clear that the partial width of the $n=2$ TES is smaller due to the smaller overlaps and R^k integrals involving the $1s$ orbital or scattering orbitals of larger energy. For example, the overlap $\langle 3s_{\mathrm{He}-}|2s_{\mathrm{He}}\rangle$ that appears in the expression for the decay of the $n=3$ TESs [it multiplies the R^0 integral $R^0(3s_{\mathrm{He}-}p_{\mathrm{He}-};3s_{\mathrm{He}}\varepsilon p)$] equals -0.0424. On the other hand, the overlap $\langle 2s_{\mathrm{He}-}|1s_{\mathrm{He}}\rangle$, which appears in the three-electron matrix element for the decay of the $n=2$ TESs, is 22 times smaller, being -0.0019.

(2) The superposition of transition amplitudes that are determined in terms of a few main configurations. This feature allows the recognition of possible cancellation effects on transition-matrix elements, such as the autoionization widths. This was first demonstrated in Refs. [16,17], in connection with the widths of the $2p3p\ ^3D$ DES of He. For example, in

TABLE V. Values of the matrix element $W=V-ES$ for each configuration of the channels He $23sp_+\ ^3P^o$ and $23sp_-\ ^1P^o$ for the three lowest triply excited resonance states of He^-, $3s^23p\ ^2P^o$, $3s3p^2\ ^4P$, and $3s3p^2\ ^2D$. V is the Coulomb interaction matrix element and S is the overlap. Comparing the numbers for the two channels, $^3P^o$ and $^1P^o$, whereas the ones for S are of the same order of magnitude, the ones for V differ considerably, showing that the $^3P^o$ channel interacts more strongly.

		V (a.u.)			S (a.u.)			W (a.u.)		
Threshold	Configuration	$^2P^o$	^4P	^2D	$^2P^o$	^4P	^2D	$^2P^o$	^4P	^2D
$23sp_+\ ^3P^o$	$2s3p$	0.0163	−0.0130	−0.0169	−0.0779	0.0901	0.0872	−0.0129	0.0207	0.0148
	$2p3s$	−0.0471	0.0499	0.0466	0.0861	−0.0818	−0.0705	−0.0147	0.0193	0.0126
	$2p3d$	0.0063	−0.0075	−0.0032	−0.0086	0.0135	0.0055	0.0031	−0.0024	−0.0012
Total		−0.0109	0.0154	0.0065	−0.0211	0.0324	0.0341	−0.0189	0.0275	0.0189
$23sp_-\ ^1P^o$	$2s3p$	−0.0022	−0.0035	−0.0005	−0.0276	0.0524	0.0411	−0.0125	0.0161	0.0145
	$2p3s$	−0.0059	0.0009	0.0022	−0.0246	0.0362	0.0300	−0.0158	0.0144	0.0131
	$2p3d$	−0.0023	−0.0005	0.0010	−0.0055	0.0090	−0.0007	−0.0044	0.0028	0.0008
Total		0.0026	−0.0024	−0.0014	0.0060	−0.0014	−0.0060	0.0049	−0.0030	−0.0036

Ref. [17] it was stated that "*the contribution to the width of the* $2p3p$ *and* $2s3d$ *configurations present in the MCHF zero-order vector, nearly cancel each other. This implies that in this case the width is determined essentially by correlation of the* $2pv_f$ *and* v_sv_d *type, where* v_l *are virtual orbitals.*"

A similar type of constructive and destructive interference can be shown to occur here with the He $^3P^o$ and $^1P^o$ channels, whose zero-order wave functions are given in Sec. IV. For example, two of the major decay matrix element for the $^3P^o$ channels are $\langle\varphi(3s^23p)\ ^2P^o|H-E|\varphi(23sp_+)\ ^3P^o\varepsilon s\rangle$ and $\langle\varphi(3s^23p)\ ^2P^o|H-E|\varphi(23sp_-)\ ^3P^o\varepsilon s\rangle$. Analysis shows that there is cancellation for the $\varphi(23sp_-)\ ^3P^o$ channel, and this is reflected on the very small width. In Table V we present values for the matrix elements that are relevant to the above discussion. W is the full matrix element whose form is $W=V-ES$. V is the Hamiltonian interaction, S is the overlap between initial and final state wave functions, and E is the energy of the resonance state. For all three states, $^2P^o$, ^4P, and ^2D, V is much larger for the components of the $\varphi(23sp_+)\ ^3P^o\varepsilon s$ channel than of the $\varphi(23sp_-)\ ^3P^o\varepsilon s$ one. At the same time, the overlaps S are of the same magnitude. The calculation of W depends on the coefficients of the final DES of He (Table I). For the component $2s3p$ of the $\varphi(23sp_+)\ ^3P^o$ vector the coefficient is almost the same and of the same sign as the one for $2p3s$ component of the $\varphi(23sp_-)\ ^3P^o$ vector. On the other hand, the coefficient of the $2p3s$ component of the $\varphi(23sp_+)\ ^3P^o$ vector is of opposite sign of that of the $2s3p$ component of the $\varphi(23sp_-)\ ^3P^o$ vector. The result is constructive interference for the $\varphi(23sp_+)\ ^3P^o$ channel and a much larger W than for the $\varphi(23sp_-)\ ^3P^o$ channel, regardless of the type of initial state.

IX. SYNOPSIS

As a continuation of our work on the analysis and computation of multiply excited resonance states within the state-specific theory, in this paper we focused on certain prototypical cases in He^-, Li, and in ions of the isoelectronic sequence, where three electrons occupy mainly the $n=3$ shell. The quantum-mechanical many-electron problem for such states is complicated by a number of factors, as, for example, is the presence of lower lying multiply excited resonance states and of a plethora of important open channels corresponding to one- and two-electron bound or quasilocalized states.

The applications were done to the $3s^23p\ ^2P^o$, $3s3p^2\ ^4P$, and $3s3p^2\ ^2D$ triply excited states. Energies as well as partial and total widths (only for He^-)—in the independent channel approximation—were computed. A test of the level of accuracy of these calculations was the determination of the position of the Li $3s^23p\ ^2P^o$ state at 175.15 eV, in very good agreement with the measured value of Diehl *et al.* [11] (175.165 ± 0.050 eV).

Our study showed that, due mainly to the effects of localized electron correlation, the $3s^23p\ ^2P^o$ state is below the ^4P state along the isoelectronic sequence, He^- included, contrary to the conclusions of Refs. [3,9] where an inversion of these two states was predicted for He^- and for N^{+4}.

As regards the computational methodology, we discussed the positive role of the OCL configurations with respect to the state orthogonality, the satisfaction of the virial theorem, and the contribution to the energy of the localized Ψ_0 of multiply excited states, when they are included in the zero-order MCHF calculation. The computation of the partial and total widths in the independent channel approximation revealed the major decay channels, namely, the He $\varphi(23sp_+)\ ^3P^o$ and the $\varphi(2s3s)\ ^1S$, and produced results in essential agreement with those of Ref. [3] for their partial widths. Disagreement is observed only for certain small partial widths. The total widths of the three states in He^- are nearly the same, around 170 meV.

Finally, it was discussed how the interplay between electronic structure and widths can be understood, heuristically as well as quantitatively, in terms of orbital overlaps and of constructive and destructive superposition of the main configurations in decay channels.

ACKNOWLEDGMENT

We thank the Empirikion Foundation, Athens, for financial support to one of us (N.A.P.).

[1] (a) C. A. Nicolaides and N. A. Piangos, Phys. Rev. A **64**, 052505 (2001), and references therein; (b) C. A. Nicolaides, N. A. Piangos, and Y. Komninos, *ibid.* **48**, 3578 (1993).
[2] C. A. Nicolaides and N. A. Piangos, J. Phys. B **34**, 99 (2001).
[3] K. T. Chung, Phys. Rev. A **64**, 052503 (2001).
[4] T. Morishita and C. D. Lin, Phys. Rev. A **64**, 052502 (2001).
[5] D. Roy, Phys. Rev. Lett. **38**, 1062 (1977).
[6] C. A. Nicolaides, Phys. Rev. A **46**, 690 (1992); M. Bylicki and C. A. Nicolaides, *ibid.* **48**, 3589 (1993).
[7] C. G. Bao, J. Phys. B **25**, 3725 (1992).
[8] Y. Komninos, M. Chrysos, and C. A. Nicolaides, Phys. Rev. A **38**, 3182 (1988); C. A. Nicolaides, M. Chrysos, and Y. Komninos, *ibid.* **41**, 5244 (1990).
[9] N. Vaeck and J. Hansen, J. Phys. B **25**, 883 (1992).
[10] H. Bachau, J. Phys. B **29**, 4365 (1996).
[11] S. Diehl *et al.*, Phys. Rev. A **56**, R1071 (1997).
[12] Y. Azuma *et al.*, Phys. Rev. Lett. **79**, 2419 (1997).
[13] E. Lindroth, Phys. Rev. A **49**, 4473 (1994).
[14] C. Froese Fischer, Comput. Phys. Commun. **14**, 145 (1978).
[15] J. W. Cooper, U. Fano, and F. Prats, Phys. Rev. Lett. **10**, 518 (1963).
[16] Y. Komninos and C. A. Nicolaides, Phys. Scr. **28**, 472 (1983).
[17] G. Aspromallis, Y. Komninos, and C. A. Nicolaides, J. Phys. B **17**, L151 (1984); G. Aspromallis and C. A. Nicolaides, *ibid.* **17**, L249 (1984).
[18] S. I. Themelis and C. A. Nicolaides, Phys. Rev. A **49**, 1618 (1994).
[19] M. Bylicki, Phys. Rev. A **39**, 3316 (1989).
[20] K. T. Chung, Phys. Rev. A **41**, 4090 (1990).
[21] Articles by D. R. Beck and C. A. Nicolaides, in *Excited States in Quantum Chemistry*, edited by C. A. Nicolaides and D. R. Beck (Reidel, Dordrecht, 1978); C. A. Nicolaides, in *Giant Resonances in Atoms, Molecules and Solids*, edited by J. P. Connerade, J. M. Esteva, and R. C. Karnatak (Plenum, New York, 1987), p. 213.
[22] Y. Komninos and C. A. Nicolaides, J. Phys. B **19**, 1701 (1986); C. A. Nicolaides, S. I. Themelis, and Y. Komninos, *ibid.* **35**, 1831 (2002).
[23] Y. Komninos, N. Makri, and C. A. Nicolaides, Z. Phys. D: At., Mol. Clusters **2**, 105 (1986).
[24] C. A. Nicolaides and D. R. Beck, Chem. Phys. Lett. **36**, 79 (1975).
[25] C. A. Nicolaides and D. R. Beck, J. Phys. B **9**, L259 (1976); C. A. Nicolaides and D. R. Beck, Chem. Phys. Lett. **53**, 87 (1975).
[26] L. B. Madsen, J. Phys. B **34**, 2134 (2001).
[27] N. A. Piangos and C. A. Nicolaides, J. Phys. B **34**, L633 (2001).
[28] Y. Zhang and K. T. Chung, Phys. Rev. A **58**, 3336 (1998).
[29] K. T. Chung, Phys. Rev. A **51**, 844 (1995).
[30] M. Bylicki and C. A. Nicolaides, Phys. Rev. A **51**, 204 (1995).
[31] K. T. Chung and B. Gou, Phys. Rev. A **52**, 3669 (1995).
[32] B. Gou and K. T. Chung, J. Phys. B **29**, 6103 (1996).